Design of an integrated electromagnetic levitation and guidance system for SwissMetro

D'Arrigo Aldo, Rufer Alfred
Swiss Federal Institute of Technology
Industrial Electronics Laboratory
1015 Lausanne, Switzerland.
Tel.: +41 693 46 76 / Fax: +41 21 693 26 00
e-mail: alfred.rufer@epfl.ch
URL: leiwww.epfl.ch

Acknowledgement

The authors gratefully acknowledge the support of S. Colombi, for his advice on this paper, and the work of all the SwissMetro project collaborators.

Keywords

Actuators, Control, Magnetic Devices, Mechatronics, Modelling, Simulation.

Abstract

Electromagnetic levitated and guided systems are commonly used in the field of people transport vehicles, tool machines frictionless bearings and conveyor systems. In the case of low speed people transport vehicles, the electromagnetic levitation offers the advantage of a very silent motion and of a reduced maintenance of the rail.

In the world there are actually two working low speed systems: the Japanese HSST ([1], [2]) and the English BAMS (Birmingham Airport MagLev System [3]). In both these magnetically levitated trains the guidance force needed to keep the vehicles on the track is obtained with the levitation electromagnets, thanks to particular shapes of the rails and to a clever placement of the electromagnets with respect to the rails ([4]).

This paper shows a simple magnetic model for the study of the levitation and guidance forces produced by an electromagnet coupled with an iron rail. The rail and electromagnet shapes taken into consideration in this paper can better refer to the Japanese HSST than to the English BAMS. This paper will also deals with the study of the guidance force in the case of a vertical position control. The study shows that the guidance force can be stronger than in an open loop study.

Study of the electromagnet-rail system

Shapes of the rail

The mechanical action we are interested to depends not only on the structure of the electromagnet but also on the shape of the rail. In particular, the same electromagnet coupled to rails of different shapes results in a change of intensity of the two forces. The shape of the rail is important, first of all in order to get levitation and guidance force with the same electromagnet.

In the case of a flat rail larger than the electromagnet, there is only a levitation force (figure 1).

Integrated guidance force can appear if we couple the electromagnet with a narrow rail, as shown in figure 2.

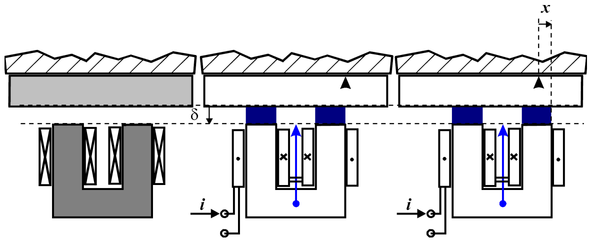

Figure 1 : Only levitation force with a flat wide rail

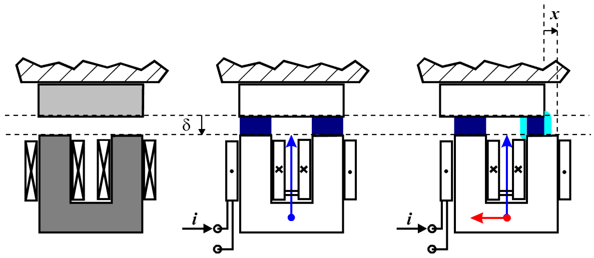

Figure 2 : Levitation and guidance forces with a flat narrow rail

Or with a C-shaped rail, as shown in figure 3.

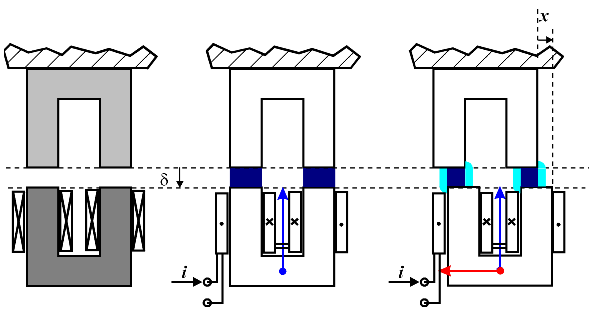

Figure 3 : Levitation and guidance forces with a C-shaped rail

What we are interested in is a mathematical model that gives us a relationship between the following variables:

i : the current flowing in the coils
x : the lateral position of the electromagnet
δ : the airgap between the electromagnet and the rail
f_{LEV} : the levitation force
f_{GUID} : the guidance force

Usually for the calculation of the guidance force complete leakage fluxes and wide fringe fluxes are usually taken into account. We would like to create a simpler magnetic model, in order to simplify the calculations of static forces and the dynamic simulations.

Magnetic model

As we know, the basis for force calculation is the study of the magnetic circuit. The simplest magnetic circuit of the system takes into account only the permeance of the two airgaps; the permeance of each airgap is a function of the distance δ and the lateral position x:

$$\lambda_{AIRGAP} = \lambda_{AIRGAP}(\delta, x) \tag{1}$$

Even the inductance, as a combination of the two permeances, will be a function of δ and x. Then the magnetic energy of the circuit will be a function of both co-ordinates and of the current flowing in the coils:

$$L(\delta, x) \quad \Rightarrow \quad e(i,\delta,x) = \frac{1}{2} L(\delta,x)\, i^2 \tag{2}$$

So we can calculate the levitation and the guidance force with the well-known formulas:

$$\left.\begin{aligned} f_{LEV}(i,\delta,x) &= \frac{1}{2}\left[\frac{\partial}{\partial\delta}L(\delta,x)\right]i^2 \\ f_{GUID}(i,\delta,x) &= \frac{1}{2}\left[\frac{\partial}{\partial x}L(\delta,x)\right]i^2 \end{aligned}\right\} \tag{3}$$

As we said before, a simple magnetic model is taken for the calculation of the forces. We neglect the magnetic potential losses in the iron parts (core and rail) and the leakage fluxes, and we assume that the magnetic flux flows in the airgaps in a constant section, for any value of δ and x. So we can think that, for a given δ, the more the electromagnet is far from the central position, the greater is the mean distance of the magnetic flux lines in the airgap.
Part of the magnetic flux will go straight in the airgap, in the so called mean reluctance, and the rest of the flux will be obliged to take a longer and partly curved path, in the two so called fringe reluctance.

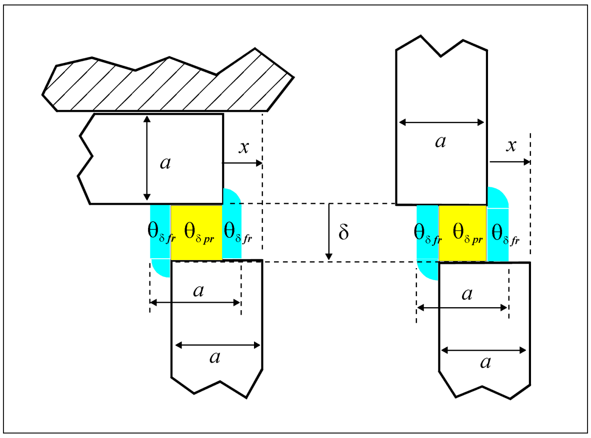

Figure 4 : Magnetic flux in the airgap

As shown in figure 4, in the case of the flat narrow rail only one airgap changes at a time. In the case of the C-shaped rail the two airgaps change for any x offset. That is why the C-shaped rail can provide a greater guidance force. Indeed the Japanese HSST has C-shaped rails [2]. Let's write the expression for the airgaps: in the case of the flat narrow rail, the two airgap geometry's are not the same, and only one airgap is changing because of a shift in x:

$$\left.\begin{aligned} \lambda_{ED}(x,\delta) &= \mu_0\left[\frac{a-x}{\delta}+\frac{4}{\pi}\ln\left(1+\frac{\pi\,x}{4\,\delta}\right)\right]l \\ \lambda_{EG}(x,\delta) &= \mu_0\,\frac{a\,l}{\delta} \qquad x\geq 0 \end{aligned}\right\} \tag{4}$$

In opposition in the U-shaped rail both airgaps change because of a shift in x: the common expression is

$$\lambda(x,\delta) = \mu_0\left[\frac{a-x}{\delta}+\frac{4}{\pi}\ln\left(1+\frac{\pi\,x}{4\,\delta}\right)\right]l \qquad x\geq 0 \tag{5}$$

Because of the symmetry of the two airgaps, the calculation of the inductance, the energy and the forces are simpler than in the case of the flat rail. So we write the expressions for the U-shaped rail only (Positive x positions; we have):

$$L(x,\delta) = N^2\,\frac{1}{2}\mu_0\left[\frac{a-x}{\delta}+\frac{4}{\pi}\ln\left(1+\frac{\pi\,x}{4\,\delta}\right)\right]l \tag{6}$$

$$f_{LEV}(x,\delta,i)=\frac{1}{4}N^2\,\mu_0\left[-\frac{(a-x)}{\delta^2}-\frac{4\,x}{4\,\delta^2+\pi\,\delta\,x}\right]l\,i^2 \tag{7}$$

$$f_{GUID}(x,\delta,i)=\frac{1}{4}N^2\,\mu_0\left[-\frac{1}{\delta}+\frac{4}{4\,\delta+\pi\,x}\right]l\,i^2 \tag{8}$$

It is easy to verify that in the case x = 0 the levitation force has the same value we can get in a simple levitation electromagnet. In this case the guidance force is zero.

Results with an example electromagnet

Dimensions and weight

The calculations we will do next use the dimensions of the electromagnet used in a new guidance system for SwissMetro project. Figure 5 shows the main values.
Around the iron core there are two windings with 187 turns; the two windings are in a series connection. This electromagnet has a total weight of 80 Kg, and we imagine that the electromagnet is loaded with a 160 Kg load. In these conditions by feeding the coils with the nominal current of 40 A the electromagnet will keep the nominal airgap to reach the nominal levitation force of about 240 Kg.

Inductance of the winding

Figure 6 shows in a 3D graphic the inductance of the system with a C-shaped rail, function of x and δ; this result is the direct representation of the equation (6).

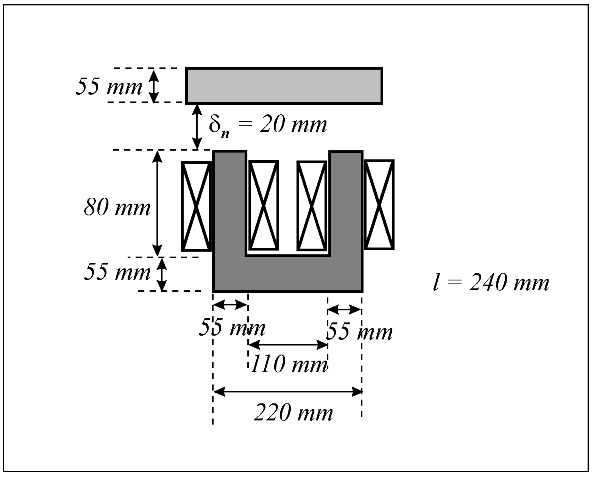

Figure 5 : Levitation and guidance magnet details

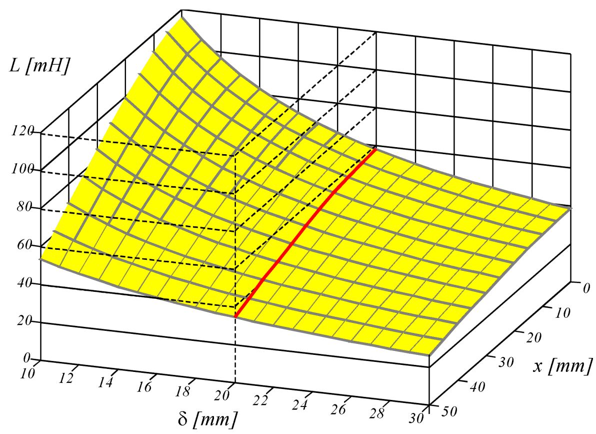

Figure 6 : Inductance of the electromagnet coupled with a C-shaped rail

For a given airgap, the inductance of the winding decreases with the x offset of the electromagnet.

Open loop levitation and guidance forces

Imagine to supply the electromagnet with a constant current: the levitation and the guidance forces depend on the position of the electromagnet, described by 'x' and 'δ'. We want to know the values of the two forces for a fixed δ and for different values of x. We compare the results of our model with the finite elements calculation (using the Flux2D package). We first consider the electromagnet coupled with a flat narrow rail. Figure 7 shows the induction in the system with the electromagnet in an offset position:

Figure 8 shows in the hatched line the results of the finite element calculation and in continuous line the results of the simple magnetic model.

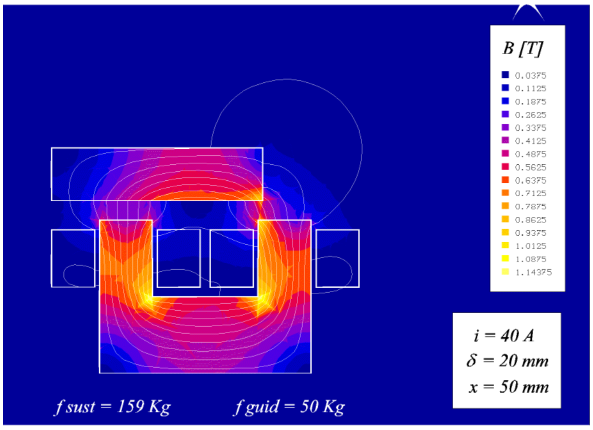

Figure 7 : Flux2D finite elements calculation for a magnet coupled with a flat narrow rail

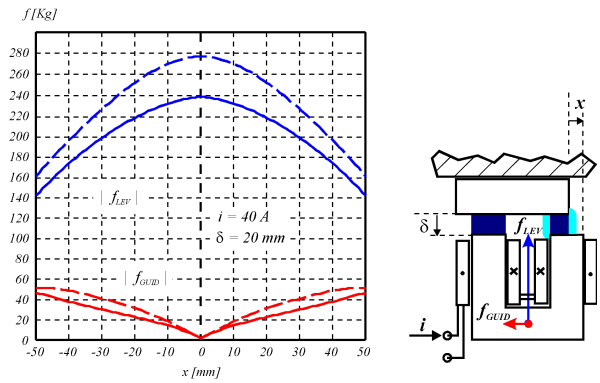

Figure 8 : Modules of levitation and guidance force with a flat narrow rail

We can notice that the levitation force is maximum when the electromagnet is centred (x = 0), whereas the guidance force is zero. The more the electromagnet is far from the central position, the lower is the levitation force, whereas the higher is the guidance force. The forces obtained with Flux2D are very close to the forces we could measure on a real rig. The difference between those forces and the forces obtained with our model is less than 20 %. The results are even better for the C-shaped rail, almost for the guidance force. First, we show in figure 9 the induction in the system with the electromagnet in an offset position.

As above, figure 10 shows in the hatched line the results of the finite element calculation and in continuous line the results of the simple magnetic model.

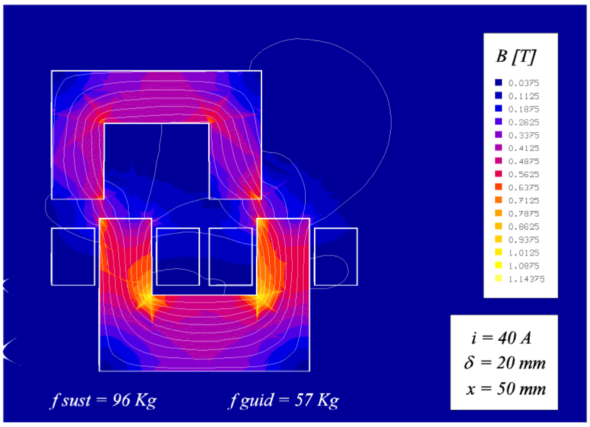

Figure 9 : Flux2D finite elements calculation for a magnet coupled with a C-shaped rail

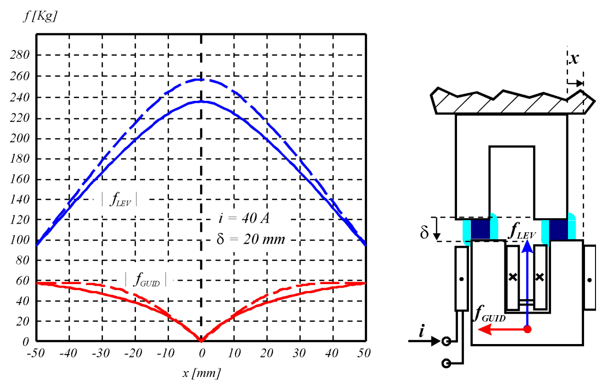

Figure 10 : Modules of levitation and guidance force with a C-shaped rail

Close loop levitation and guidance forces

It is clear that the open loop calculation doesn't take into account all the features of the real application. Even in the case of no disturbance the electromagnets have to support a constant vertical force due to the weight of the vehicle. As the electromagnets are the actuators of a levitation system that aims to hold a constant vertical position δ, they must provide constant levitation force. If we study the guidance force in these working conditions, we can notice that the guidance force is higher than in the previous evaluations.

The difference between the closed loop and the open loop guidance force is about twice for the flat narrow rail coupling and more than twice for the C-shaped rail coupling. In figure 11 we show the result for the flat rail: the guidance force and the current needed to provide the guidance force.

In figure 12 we show the result for the C-shaped rail: again the guidance force and the current needed to provide the guidance force. Even in close loop calculation the C-shaped rail is better than the flat rail; it can give with the same electromagnet twice the guidance force as the flat rail.

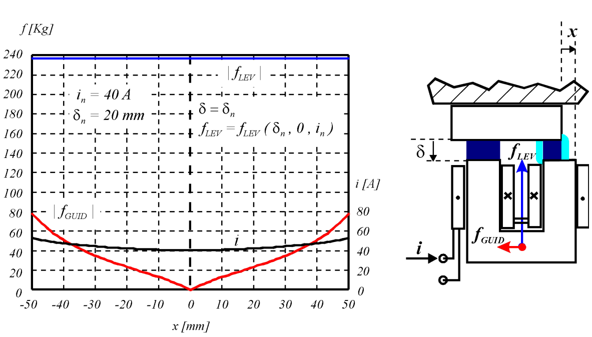

Figure 11: Module of guidance force and current for a constant levitation force operating with a flat narrow rail

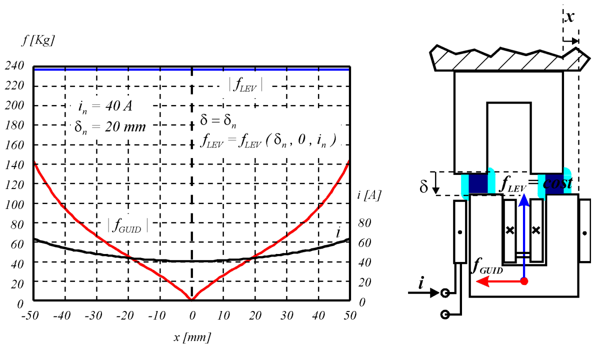

Figure 12 : Module of guidance force and current for a constant levitation force operating with a C-shaped rail

Changing the value of the airgap

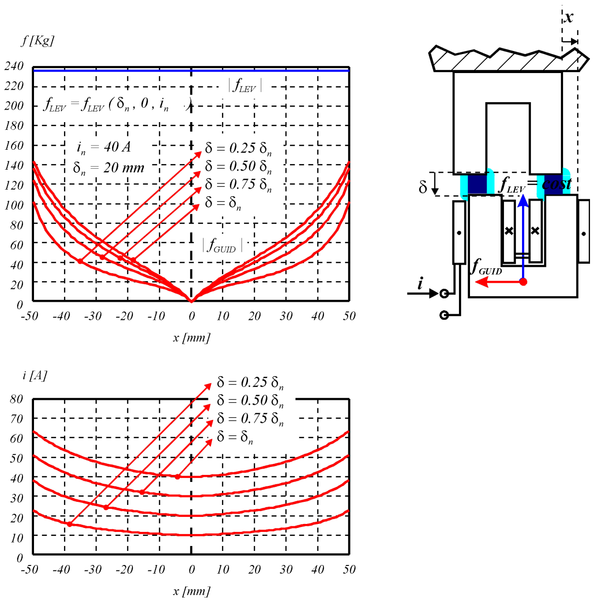

Figure 13 : Module of guidance force and current for a constant levitation force operating at different airgap values (C-shaped rail)

The closed loop levitation characteristics represented in the previous paragraph for the two types of rail have been obtained with a 20 mm airgap. How does the characteristic change if we keep a constant levitation force and we change the airgap?

We will only consider the case of the coupling of the electromagnet with a C-shaped rail. In figure 13 we plot the curves of the guidance force and the current in the coils for different airgaps. A smaller airgap results in a weaker guidance force. We can notice that the slope of the curves for x=0 is always the same for different airgaps.

Lateral behaviour of the integrated levitation and guidance electromagnet

As we can see in the close loop forces diagrams (figures 11, 12 and 13) the lateral response of the electromagnet due to the airgap control is a force increasing with the lateral offset; this force is almost a linear function of the lateral offset of the electromagnet. Then we can imagine that the electromagnet will move laterally as a mass bound by a spring. As we know, a spring working on a mass is a mechanical resonant system, whose resonance frequency is given by:

$$f_{RES} = \frac{1}{2\pi}\sqrt{\frac{K_{GUID}}{M}} \tag{9}$$

where the M is the sum of the masses of the electromagnet and of part of the carried vehicle. We can easily imagine that any external action will cause a non-dumped oscillating response of the lateral position. The value of K_{GUID} can be taken from the figure 12, as a mean value of the slope of the closed loop guidance characteristic. The stiffness value of the guidance can also be evaluated by the x-derivative of the open loop guidance force; the slope of the two characteristics for x=0 is the same. Here is the formula:

$$\frac{\partial}{\partial x} f_{GUID}(x,\delta,i) = \frac{1}{4} N^2 \mu_0 \left[-\frac{4\pi}{(4\,\delta + \pi\, x)^2} \right] l\, i^2 \qquad x \geq 0 \tag{10}$$

and by evaluating this derivative in the central position, with nominal airgap and current:

$$K_{GUID} = \frac{\partial f_{GUID}}{\partial x}(0,\delta_n,i_n) = \frac{\pi}{16}\mu_0\, l\, (N\, i_n)^2 \frac{1}{\delta_n^2} \tag{11}$$

We can notice that the only mechanical dimension is appearing in (11) is the length, and the guidance stiffness is proportional to this length. That is why the Japanese HSST uses long electromagnets.

For a given electromagnet, the equivalent spring stiffness increases with the square of the current and decreases with the ratio of the airgap. For our system the resonance frequency is around 2 Hz; for any real magnetic levitation system this frequency will always be between 1 and 10 Hz.

The lateral mechanical resonance is the main drawback of an integrated levitation and guidance system. The two existing transport systems based on this kind of technology, the Japanese HSST and the English Birmingham Airport Project, both solve this problem by splitting each levitation unit in two electromagnets with a separate regulated supply.

The two electromagnets of each pair are laterally offset on opposite sides relative to the U-shaped rail centre line ([3], [4] and [5]). The electromagnets pairs are supplied together to give vertical control and guidance, and differentially to introduce lateral damping.

Dynamic simulations

Up to now, we have developed algebraic and differential calculations for the steady state. These results must be validated to check the dynamic behaviour. For this, we have implemented the 5th order system in a MatLab Simulink file. Figure 14 shows the mechanical system. The electromagnet has a PWM current control.

As we know the relationship among x, δ, i and f_{LEV} if we measure the airgap and the lateral offset, we can calculate the reference current to give to the current loop to obtain the reference force value. So the levitation force control is based on the measure of the electromagnet position. The guidance force is not controlled. Finally the airgap control is obtained with a state feedback, as shown in figure 15 ([6] and [7]).

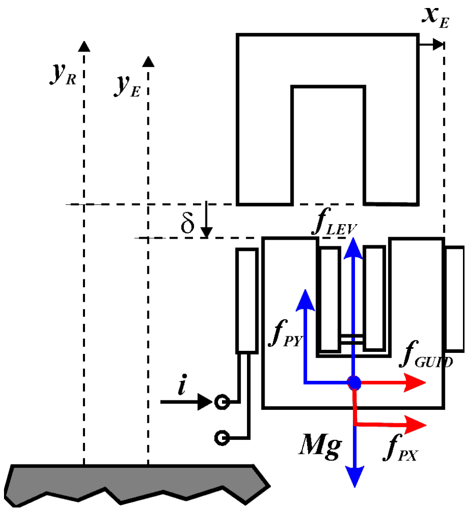

Figure 14 : Mechanical model of the system

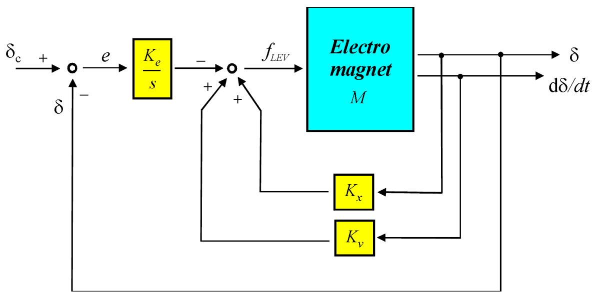

Figure 15 : Airgap control system

Power on with an initial lateral offset

As a first simulation we study the dynamic response at the power on; the initial airgap is 50 mm, and 50 mm is also the initial x shift. In figure 16 we can see that the electromagnet reaches the reference value airgap, but it oscillates in the lateral position.

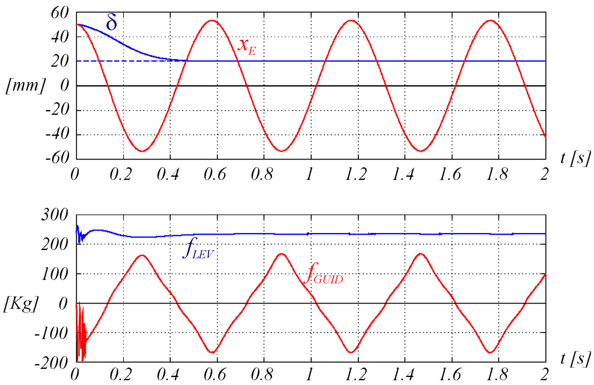

Figure 16 : Power on dynamic response to a lateral offset

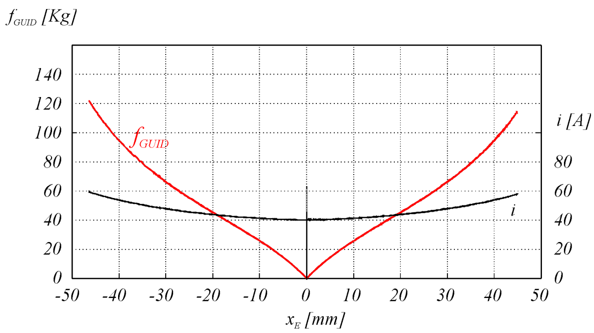

Figure 17 : Dynamic guidance characteristic

In figure 17 we plot the dynamic characteristic of the electromagnet using the variable values from the power on simulation. We can notice that the guidance force and the current in the coils are exactly the same as obtained with the static calculations and showed in figure 12.

This is normal, because the force control is much faster than the mechanical time constants of the system.

Response to a lateral sinus external force

Figure 18 shows the dynamic response to a lateral sinus force. The system is unstable, as we can see from the increasing x, but the airgap does not react to the lateral disturbing force.

Response to a lateral constant external force

If we push laterally the electromagnet with a constant force (we let the force increase linearly from zero to its constant value) the electromagnet oscillates around a shifted position depending on the value of the external force. This is represented in figure 19.

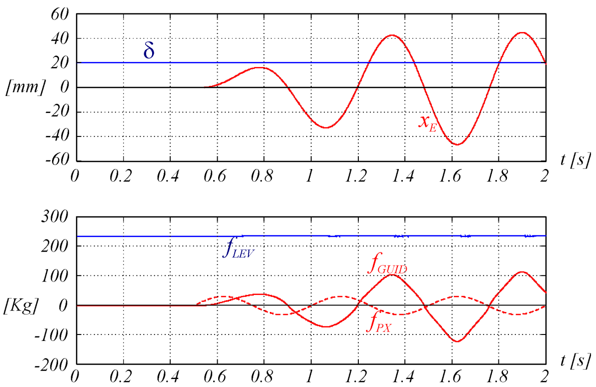

Figure 18 : Dynamic response to an external sinus force

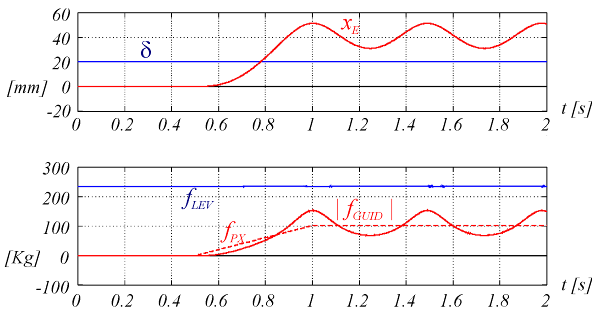

Figure 19 : Dynamic response to an external constant force

Conclusions

The theoretical study summarised in this paper shows that a simple magnetic model for levitation electromagnets can well describe the static and dynamic behaviour of the electromagnet. The result evidence the better guidance force obtained with a C-shaped rail. The next stage will be the experimental validation of these results on a full size magnetic levitation system.

References

1. Seki, Tomohiro. *The Development of HSST-100L,* Proceedings MAGLEV'95, pp 51-55.
2. Masaaki Fujino, Takeshi Mizuma. *Total test operation of HSST-100 and planning project in Nagoya,* Proceedings MAGLEV'95, pp 129-133.
3. V.Nenadovic, E. E. Riches.*MagLev at Birmingham Airport: from system concept to successful operation,* GEC Review, Vol 1, No 1, 1985, pp 3-17.
4. R. D. Fruechte, R. H. Nelson, T. A. Radomski. *Power conditioning system for a magnetically levitated test vehicle,* IEEE transaction on vehicular technology, Vol VT-29, No 1, Feb 1980, pp 50-60.
5. Y. Hikasa, Y. Takeuchi. *Detail and experimental results of ferromagnetic levitation system of Japan Air Lines HSST-01/-02 vehicles,* IEEE transaction on vehicular technology, Vol VT-29, No 1, Feb 1980, pp 35-41.
6. M. Zayadine. *Etude de réglage en position de la sustentation magnétique par attraction*, Thèse EPFL n. 1508, EPFL-LEI, Lausanne, 1996.
7. M. Zayadine, S. Colombi. *Active Control of a Magnetic Suspension System,* International Symposium MV2 on Active Control in Mechanical Engineering, pp 281-294, Hermes, Paris, 1995.
8. K. Heinrich, R. Kretzschmar. *Magnetbahn Transrapid die neue Dimension des Reisens*, Hestra-Verlag, Darmstadt, 1989.

9. B. V. Jayawant. *Electromagnetic suspension and levitation techniques*, Proc. R. Soc. Lond. A 416, pp 245-320, 1988.

10. P.-J. Riedo. *Adaptation continue des coefficients de réglage*, Bulletin ASSPA, 1986-2.

11. J. E. Paddison, R. M. Goodall. *EMS Maglev Suspension Control System Comparison and Trends*, MAGLEV'98, Mt. Fuji, Japan, 1998.